



Article

Quantification of Urban Greenspace in Shenzhen Based on Remote Sensing Data

Yu Bai ^{1,2} , Menghang Liu ^{2,3} , Weimin Wang ^{4,5,6,*}, Xiangyun Xiong ^{4,5,6} and Shenggong Li ^{1,7}

- ¹ Key Laboratory of Ecosystem Network Observation and Modeling, Institute of Geographic Sciences and Natural Resources Research, Chinese Academy of Sciences, Beijing 100101, China; lisg@igsnrr.ac.cn (S.L.)
- ² University of Chinese Academy of Sciences, Beijing 100190, China
- ³ Key Laboratory of Regional Sustainable Development Modeling, Institute of Geographic Sciences and Natural Resources Research, Chinese Academy of Sciences, Beijing 100101, China
- ⁴ Shenzhen Ecological Environmental Monitoring Center of Guangdong Province, Shenzhen 518049, China
- ⁵ Guangdong Greater Bay Area, Change and Comprehensive Treatment of Regional Ecology and Environment, National Observation and Research Station, Shenzhen 523722, China
- ⁶ State Environmental Protection Scientific Observation and Research Station for Ecology and Environment of Rapid Urbanization Region, Shenzhen 518000, China
- ⁷ College of Resources and Environment, University of Chinese Academy of Sciences, Beijing 100190, China
- * Correspondence: wang.weimin@iee.org

Abstract: Rapid urbanization has led to the expansion of Shenzhen's built-up land and a substantial reduction in urban greenspace (UG). However, the changes in UG in Shenzhen are not well understood. Here, we utilized long-time-series land cover data and the Normalized Difference Vegetation Index (NDVI) as a proxy for greenspace quality to systematically analyze changes in the spatio-temporal pattern and the exposure and inequality of UG in Shenzhen. The results indicate that the UG area has been decreasing over the years, although the rate of decrease has slowed in recent years. The UG NDVI trend exhibited some seasonal variations, with a noticeable decreasing trend in spring, particularly in the eastern part of Shenzhen. Greenspace exposure gradually increased from west to east, with Dapeng and Pingshan having the highest greenspace exposure regardless of the season. Over the past two decades, inequality in greenspace exposure has gradually decreased during periods of urban construction in Shenzhen, with the fastest rate of decrease in spring and the slowest rate of decrease in summer. These findings provide a scientific basis for a better understanding of the current status of UG in Shenzhen and promote the healthy development of the city. Additionally, this study provides scientific evidence and insights for relevant decision-making institutions.

Keywords: urban greenspace; greenspace exposure; greenspace inequality; Shenzhen



Citation: Bai, Y.; Liu, M.; Wang, W.; Xiong, X.; Li, S. Quantification of Urban Greenspace in Shenzhen Based on Remote Sensing Data.

Remote Sens. **2023**, *15*, 4957. <https://doi.org/10.3390/rs15204957>

Academic Editors: Yuji Murayama, Lei Ma and Aolin Jia

Received: 29 August 2023

Revised: 5 October 2023

Accepted: 11 October 2023

Published: 13 October 2023



Copyright: © 2023 by the authors. Licensee MDPI, Basel, Switzerland. This article is an open access article distributed under the terms and conditions of the Creative Commons Attribution (CC BY) license (<https://creativecommons.org/licenses/by/4.0/>).

1. Introduction

Rapid urbanization has led to profound changes in urban land and a higher proportion of impervious surfaces, affecting ecosystem functions and degrading the quality of biological habitats [1–5]. In recent years, the contradiction between economic development and urban ecological protection brought about through urban development has also gradually increased. Currently, many cities face a common problem: the urban heat island effect, which affects not only the ecological environment but also the quality of life of urban residents [6–9]. The establishment of healthy cities has emerged as a pivotal approach for achieving the goal of sustainable urban and community development [10–12]. As urban populations continue to grow, so do concerns regarding the livability of urban environments [13].

As an important part of a healthy city, urban greenspace (UG) plays an important role in mitigating the urban heat island effect [14,15]. In addition, UG enhances the urban ecological environment and promotes the physical and mental well-being of urban

residents [16–18]. Over the past few years, numerous studies have been conducted on the layouts, development, and benefits of UG [19–21]. However, as cities continue to develop, the existing UGs face potential encroachment, necessitating ongoing research to ensure their preservation. Additionally, the mismatch between the spatial pattern of UG and the population results in different amounts of greenspace providing ecosystem services that can be enjoyed by people in different locations in the city. Environmental inequalities caused by urbanization have garnered increasing attention from ecologists and policy makers. For example, Chen et al. discovered substantial disparities in greenspace exposure between cities in the Global South and North, with cities in the Global South having only one-third the level of greenspace exposure of cities in the Global North [22]. Similarly, in China, most cities are affected by high inequality in UG exposure [23]. Therefore, a comprehensive understanding of the patterns and modes of UG is crucial for the rational planning of urban construction, promotion of environmental equity, and improvement of human living comfort.

Since the earliest special economic zone was established in 1978, Shenzhen has undergone extensive urbanization [24–26]. This rapid urban expansion has resulted in a substantial increase in impermeable surfaces and a notable decrease in UG. Due to the rapid expansion of urban construction land and the continuous reduction in the total amount of urban natural ecological space, Shenzhen is currently facing the double pressure of urban development and ecological preservation [27]. Consequently, scholars have engaged in extensive discussions on quantifying the ecological and environmental challenges brought about by urbanization and achieving sustainable development in Shenzhen [28–31]. In the context of Shenzhen's rapid urbanization, Peng et al. discovered considerable degradation in urban ecosystem health, with substantial spatial heterogeneity [32]. Li et al. assessed the services provided by forests within Shenzhen's urban ecosystems and identified notable spatial heterogeneity in the supply of, and demand for, thermoregulatory services [7]. Qian et al. examined the impact of urban growth patterns on UG [33]. Zhang et al. utilized multiple data sources to assess the accessibility of UG in Shenzhen and discovered that non-elderly individuals are more vulnerable to environmental justice issues [34]. In addition, some studies have focused on assessing the potential of green roofs in Shenzhen using multi-source data to identify suitable areas for implementation [35]. Although studies have recently investigated the UG of Shenzhen, few studies have systematically analyzed it from a long-time-series perspective. To date, ground data are the most accurate method for determining the condition of UG, but the limited amount of such data and the lack of continuous time measurements make it difficult to apply ground field measurements directly to time-series analysis on the regional scale. Remote sensing data can provide large-area, continuous-time-series ground information, which provides a good opportunity to analyze UG changes in Shenzhen over the past two decades from a macroscopic perspective. Meanwhile, considering the changes in land cover and the spatiotemporal changes in population distribution, there are limited reports on the analysis of greenspace exposure and inequality among Shenzhen residents. Driven by the spatiotemporal changes in human distribution, UG exposure and inequality have changed over the past few decades. It is not known how UG exposure and inequality regarding UG exposure have changed in Shenzhen. In addition, the effects of vegetation seasonality on the degree of UG exposure and inequality require further investigation.

To address these emergent issues, in this study, we utilized long-time-series (2000–2020) remote sensing data to comprehensively assess the dynamics of UG in Shenzhen in terms of spatiotemporal and seasonal differences. The main objectives of this study were to (1) investigate the patterns and analyze the spatiotemporal trends of UG in Shenzhen, (2) compare the level of UG exposure across different areas within Shenzhen, and (3) examine the inequality of UG in Shenzhen.

2. Materials and Methods

2.1. Study Area

Shenzhen (113°43' to 114°38'E, 22°24' to 22°52'N) is located in the southern part of Guangdong Province, adjacent to Hong Kong (Figure 1). Shenzhen is China's first special economic zone, which has gradually developed into China's most influential and best-constructed special economic zone over the course of 40 years. Shenzhen's GDP is just below that of Shanghai and Beijing, and it ranks third in China. Shenzhen has an administrative area of 1997 square kilometers and a population of 17.68 million. Currently, Shenzhen has nine administrative districts (Futian, Luohu, Nanshan, Yantian, Baoan, Longgang, Longhua, Pingshan, and Guangming) and one functional district (Dapeng). Shenzhen has a tropical monsoon climate characterized by long summers and short winters. The climate is mild, with abundant rainfall (April–September is considered the rainy season) and sufficient sunshine. In terms of terrain, Shenzhen is higher in the southeast and lower in the northwest, with most of its land consisting of low hilly areas.

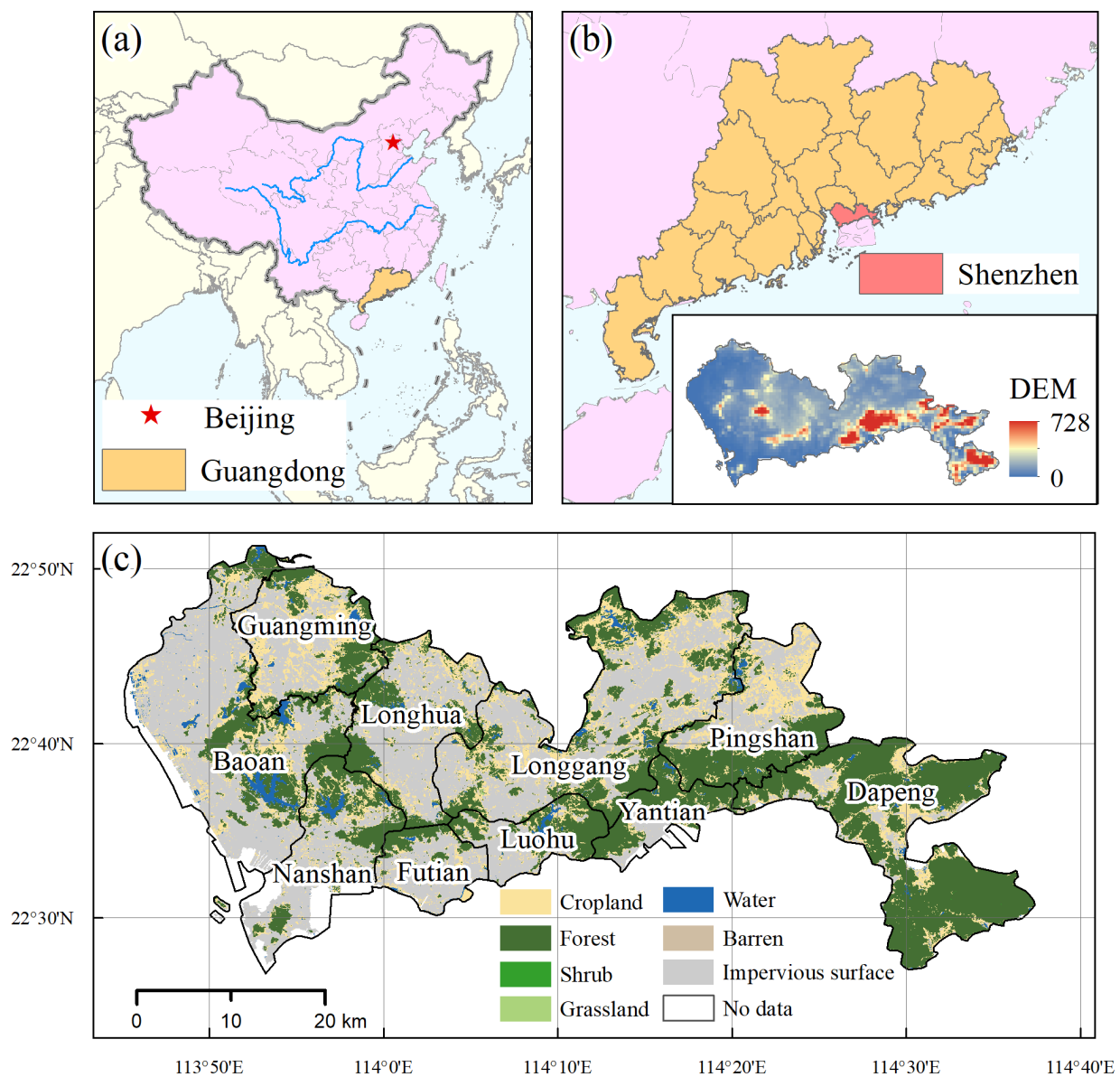


Figure 1. (a) The location of Guangdong. (b) The location and elevation of Shenzhen (data source: Global Multi-Resolution Terrain Elevation Data 2010). (c) Land cover of Shenzhen (data source: China Land Cover Dataset 2020).

2.2. Data

2.2.1. Land Cover

The land cover data used in this study were obtained from the China Land Cover Dataset (CLCD), derived from Landsat imagery, and provide annual land cover data for more than 30 years during 1990–2022 at a spatial resolution of 30 m [36]. In terms of land use, the dataset was divided into nine categories: cropland, forest, shrub, grassland, water, snow/ice, barren, impervious, and wetland. For this study, we adopted a broad definition of UG, encompassing all vegetation-covered areas within the city [37], which allowed us to systematically explore the spatiotemporal changes in the UG of Shenzhen.

2.2.2. Normalized Difference Vegetation Index (NDVI)

The NDVI is a parameter that quantifies the greenness of vegetation obtained using specific combinations of different bands and is commonly used to measure the intensity of photosynthetic activity [38]. Because of its extensive spatial coverage and long time series, the NDVI is frequently employed to assess changes in UG. Moreover, the NDVI enables the quantification of UG quality on the pixel scale. In this study, we used the Chinese regional NDVI dataset produced by Gao et al., which was generated based on the MOD13Q1 product and underwent several preprocessing steps to enhance the data quality (the preliminary reconstruction of noisy pixels with similar features from single-period imagery, Savitzky–Golay (S-G) filtering of long-time-series imagery, retention of high-quality pixels, and 16-day monthly compositing) [39]. The dataset has a spatial resolution of 250 m and a temporal resolution of monthly intervals. It covers the period from 2000 to 2022 and can be downloaded from <https://data.tpdc.ac.cn/zh-hans/data/10535b0b-8502-4465-bc53-78bcf24387b3>, accessed on 10 July 2023. In addition, the maximum value composition (MVC) method was used to generate NDVI data for each season.

2.2.3. Population

The population data used in this study were obtained from WorldPop, which is based on the WorldPop Open Population Repository, using the Random Forest method. It provides annual grid data with two spatial resolutions of 100 m and 1 km. It is widely used in geoscience research owing to its high spatial and temporal resolution and its high accuracy [22,23,40]. It is available at <https://hub.worldpop.org/project/categories?id=3>, accessed on 10 March 2023. In this study, we used the population of the Chinese region from 2000 to 2020, with a spatial resolution of 100 m.

2.3. Methods

2.3.1. Assessment of Urban Greenspace (UG) Coverage

Greenspace coverage (GC) is the ratio of greenspace to the total surface area of a city or region. The GC of the study area was calculated by determining the ratio of the UG area to the total study area. Therefore, the GC can be expressed as:

$$GC = \frac{\sum_{i=1}^n G_i}{N}, \quad (1)$$

where G_i is the GC of the i th grid, and N is the total pixel number of the study unit.

In this study, the greenspace coverage for each study unit was calculated based on the CLCD land cover dataset.

2.3.2. Assessment of NDVI Trend in UG

Sen's slope estimator and the Mann–Kendall (MK) test were used to quantify the change trend of the NDVI in UG [41,42]. These methods have been extensively utilized in geoscience research for trend analyses [43–46]. The formula can be expressed as:

$$\beta = \text{median} \left(\frac{x_j - x_i}{j - i} \right) \forall j > i \quad (2)$$

where β represents the NDVI trend of UG; x_i and x_j are NDVI values for times i and j , respectively. When β is greater than 0, it indicates an upward trend in the NDVI, while when β is less than 0, it indicates a downward trend. The method was used to calculate the NDVI trend in the study area on a pixel-by-pixel basis for the period of 2000–2020.

2.3.3. Assessment of Urban-Population-Weighted Greenspace Exposure

Population-weighted exposure modeling is a bottom-up assessment method that quantifies the interaction between a population distribution and study elements [47,48] and has been widely used in several previous studies [49–53]. Considering the population density and distribution of UG, we used urban population weighting to calculate UG exposure. The spatial interactions between the population and UG distribution can be quantified using this method. This can be calculated as follows:

$$\text{PGE} = \frac{\sum_{i=1}^n \text{Pop}_i \cdot \text{GC}_i}{\sum_{i=1}^n \text{Pop}_i} \quad (3)$$

where PGE represents the population-weighted UG exposure in a specific unit, Pop_i is the population in grid i , and GC_i is the greenspace coverage for grid i . n is the number of grids in the corresponding region.

These analyses were conducted in ArcGIS 10.8 for Windows.

2.3.4. Assessment of Inequality in Urban Population-Weighted Greenspace Exposure

Based on previous studies conducted by Song et al., we employed the Gini index to characterize the inequality in UG exposure across various regions of Shenzhen [37]. The Gini index was calculated based on the Lorenz curve, which was the UG exposure distribution curve used in this study. The specific calculations are as follows:

$$\text{Gini} = \frac{A}{A + B} \quad (4)$$

$$B = \frac{\sum_{k=1}^n (P_k + P_{k-1})(S_k - S_{k-1})}{2} \quad (5)$$

where A represents the area enclosed by the Lorenz curve and the line of absolute equity. B represents the area below the Lorenz curve enclosed by the line of absolute inequality. n is the amount of UG acquired by an individual, with k ranging from 1 to n . P_k is the cumulative proportion of the population, and $P_0 = 0$ and $P_n = 1$. S_k is the cumulative proportion of UG acquired by the corresponding population, and $S_0 = 0$ and $S_n = 1$.

The area enclosed between the line of absolute equity and coordinate axis was 50% of the total area. Therefore, A can also be expressed as:

$$A = 0.5 - B \quad (6)$$

Therefore,

$$\text{Gini} = \frac{0.5 - B}{0.5 - B + B} = 1 - 2B = 1 - \sum_{k=1}^n (P_k + P_{k-1})(S_k - S_{k-1}) \quad (7)$$

The Gini index ranges from 0 to 1, where a value closer to 0 indicates a more equal greenspace distribution, and vice versa.

3. Results

3.1. Spatiotemporal Changes in Urban Greenspace in Shenzhen

Figure 2 illustrates the changes in greenspace coverage (GC) in Shenzhen from 2000 to 2020. Shenzhen's GC decreased from 69.8% in 2000 to 55.3% in 2020 at an annual rate of -0.00701 ($p < 0.01$). The district with the highest GC was Dapeng ($>90\%$). The GC in Futian has always been low. Except for Dapeng, where the GC change was minimal, the rest of the districts showed a decreasing trend, and the rate of decline was initially fast and then slowed down. Among these districts, Longhua experienced the fastest decline in GC, dropping from 72.1% to 43.6%. Before 2008, the lowest GC value was observed in Futian. Meanwhile, the GC in Baoan sharply decreased from 0.506 in 2000 to 0.383 in 2008, making Baoan the lowest GC district after 2009.

$$\text{Trend}_{\text{Shenzhen}} = -0.00701 \quad p < 0.01$$

$$\text{Trend}_{\text{Longhua}} = -0.01421 \quad p < 0.01 \quad \text{Trend}_{\text{Guangming}} = -0.01094 \quad p < 0.01$$

$$\text{Trend}_{\text{Pingshan}} = -0.00821 \quad p < 0.01 \quad \text{Trend}_{\text{Longgang}} = -0.00975 \quad p < 0.01$$

$$\text{Trend}_{\text{Baoan}} = -0.00712 \quad p < 0.01 \quad \text{Trend}_{\text{Nanshan}} = -0.00496 \quad p < 0.01$$

$$\text{Trend}_{\text{Futian}} = -0.00300 \quad p < 0.01 \quad \text{Trend}_{\text{Yantian}} = -0.00291 \quad p < 0.01$$

$$\text{Trend}_{\text{Luohu}} = -0.00147 \quad p < 0.01 \quad \text{Trend}_{\text{Dapeng}} = -0.00082 \quad p < 0.01$$

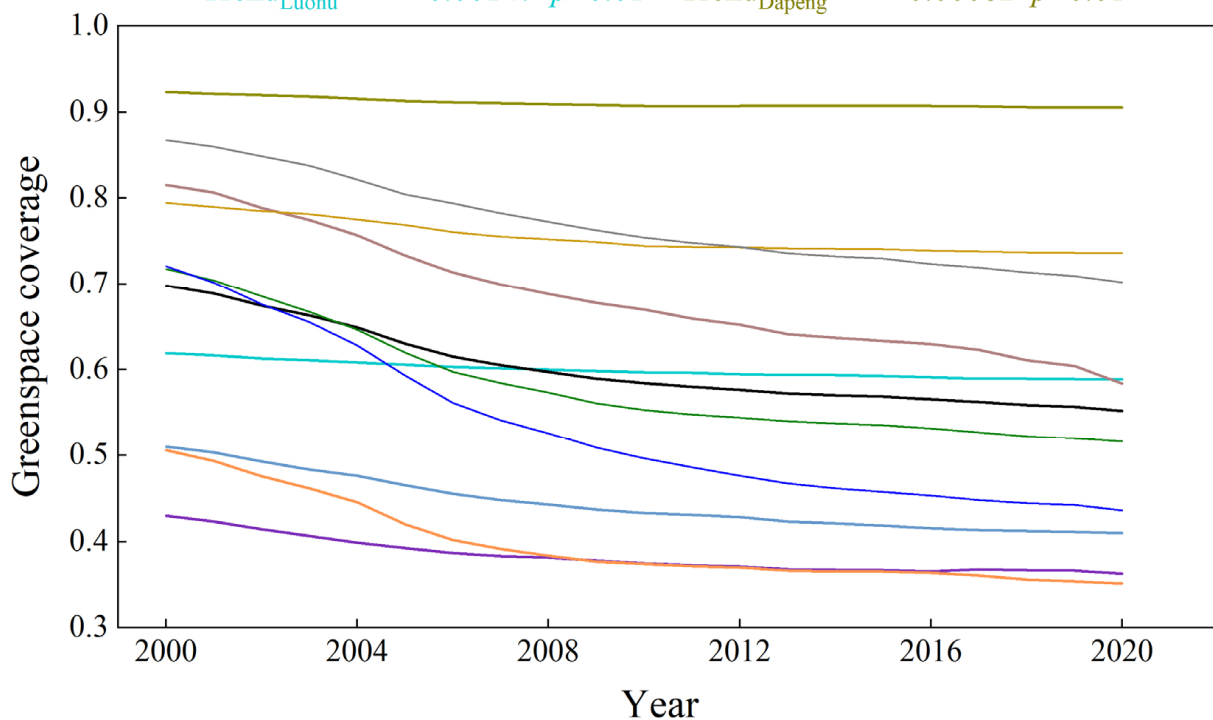


Figure 2. Changes in the urban greenspace (UG) coverage of Shenzhen and its ten districts (Futian, Luohu, Nanshan, Yantian, Baoan, Longgang, Longhua, Pingshan, Guangming, and Dapeng) from 2000 to 2020.

Figures 3 and A1, show the distribution of UG in Shenzhen from 2000 to 2020. The UG in Shenzhen gradually increased from west to east, and the reduction in UG in the west was much greater than that in the east. Since 2000, Baoan and Nanshan, in southwest Shenzhen, have seen the greatest reduction in UG, whereas in Yantian, Pingshan, and Dapeng, UG protection is better. In addition, the UG reductions in Guangming, Longhua, and Longgang were also significant. In the past 20 years, the rate of decrease in UG has changed from fast to slow, and it has stabilized in recent years.

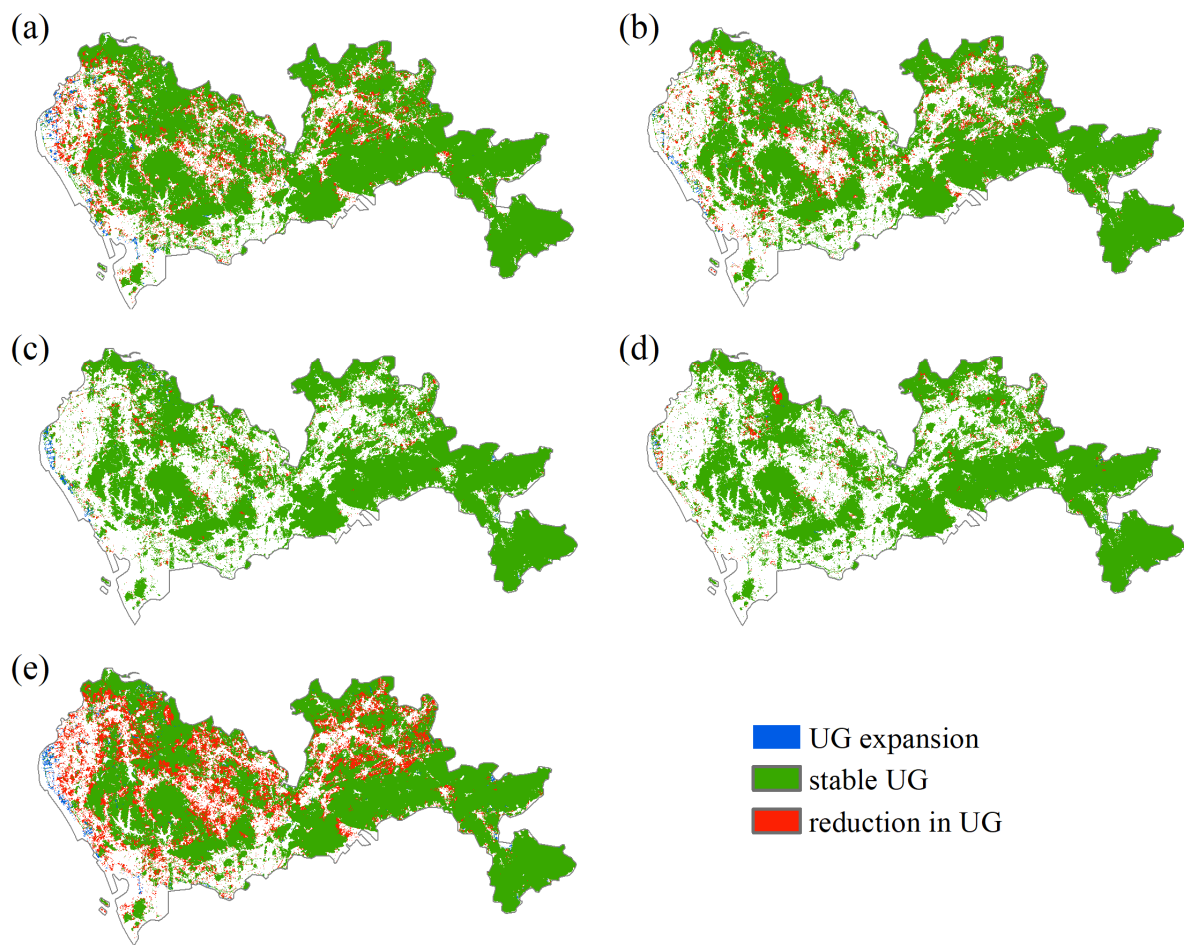


Figure 3. The spatial distribution of UG in Shenzhen in (a) 2000–2005, (b) 2005–2010, (c) 2010–2015, (d) 2015–2020, and (e) 2000–2020.

Figure 4 shows the mean NDVI of UG (stable UG for 21 consecutive years) in different seasons and its trend from 2000 to 2020. Regardless of season, the eastern part of Shenzhen exhibited higher NDVI values than the western part. The areas with higher NDVI values in the west were primarily concentrated at the junction of Baoan, Longhua, and Nanshan in Yangtai Mountain National Forest Park. In addition to summer (June–July–August, JJA), we found that the NDVI was also high in autumn (September–October–November, SON). Throughout the year, UG’s NDVI was the lowest in spring (March–April–May, MAM). Our study revealed significant spatial heterogeneity in the NDVI trend of UG in Shenzhen, with some areas exhibiting opposite trends. The areas with faster rates of decline were mainly concentrated in the areas of Fenghuang Mountain in Baoan, Tiegang Reservoir in Baoan, and Dashukeng Reservoir in Longhua. The trend of decline also varied across seasons, with the most significant decrease in the NDVI occurring in MAM, and the decreased area accounted for approximately 25.2% of the total area (the significant area was 20.9%). In winter, the NDVI increased the most, accounting for approximately 90.3% of the total area (the significant area was 16.6%). Notably, Guangming consistently showed a decreasing NDVI trend, regardless of the season.

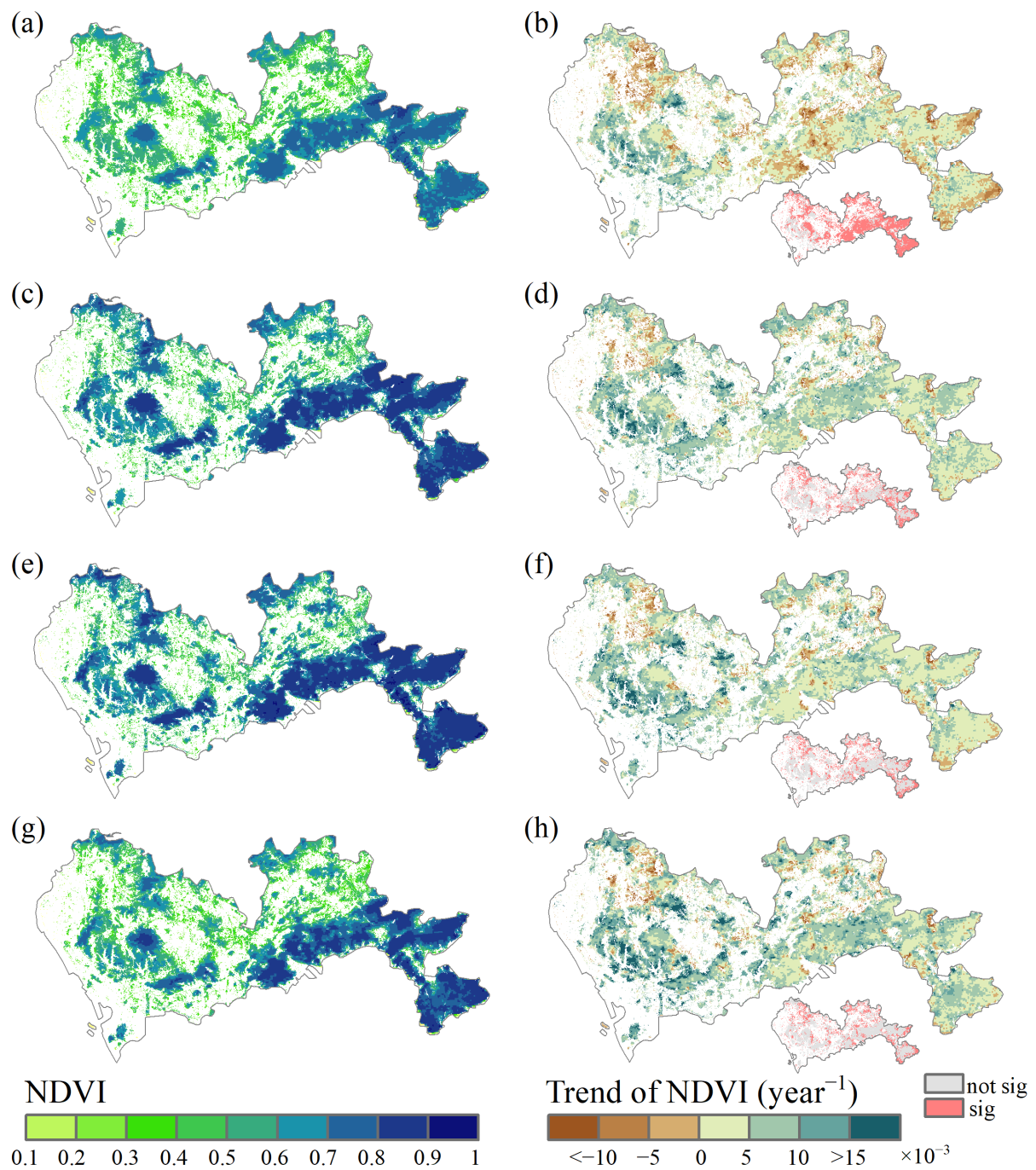


Figure 4. The spatial pattern of seasonal-averaged NDVI and NDVI trends in (a,b) MAM, (c,d) JJA, (e,f) SON, and (g,h) DJF (December–January–February, winter) from 2000 to 2020 (these maps only display the pixels that represent UG and have remained unchanged for 21 consecutive years from 2000 to 2020).

3.2. Urban Greenspace Exposure in Shenzhen

To explore seasonal differences in UG exposure, we quantified UG exposure in MAM, JJA, SON, and DJF in Shenzhen from 2000 to 2020 (Figure 5). Overall, the UG exposure was higher in SON (average: 0.047; range: 0.041 to 0.053) and JJA (average: 0.045; range: 0.038 to 0.050) than in DJF (average: 0.039; range: 0.031 to 0.047) and MAM (average: 0.037; range: 0.029 to 0.044). However, UG exposure varied across different locations, generally decreasing from west to east. Dapeng had the highest UG exposure, followed by Pingshan,

and Baoan had the lowest UG exposure. The highest value of UG exposure was found for Dapeng in SON (average: 0.082; range: 0.076 to 0.089), whereas the lowest value was found for Baoan in MAM (average: 0.025; range: 0.018 to 0.034).

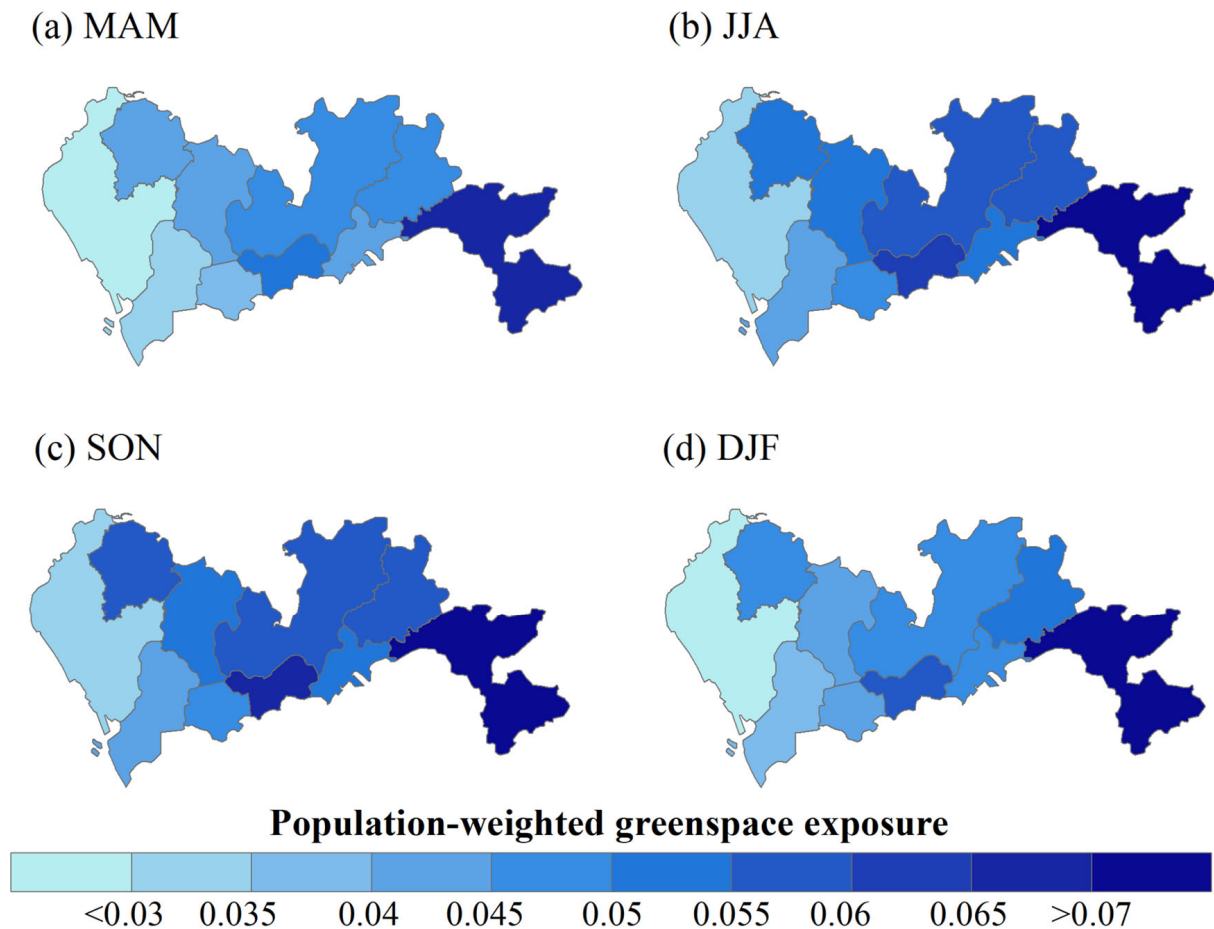


Figure 5. The annual average population-weighted UG exposure during 2000–2020 in (a) MAM, (b) JJA, (c) SON, and (d) DJF.

In the past 20 years, the UG exposure of Shenzhen has shown an upward trend in all seasons and is significant at the 0.01 level (Figure 6). However, there were significant spatial discrepancies among the different districts in terms of UG exposure. For example, in MAM, there was a downward trend in Luohu and Yantian and an insignificant upward trend in Dapeng and Pingshan, which was not consistent with the overall pattern in Shenzhen. Although UG exposure was higher in MAM and SON than in DJF, it increased the fastest in DJF. In addition, while UG exposure in Shenzhen increased, there is a slight but not significant decreasing trend observed in Yantian and Guangming. Notably, while the southeastern region had the highest UG exposure, the rate of increase was smaller than that in other areas. By contrast, Nanshan, Futian, and Longhua exhibited faster growth rates. In particular, the UG exposure trend for Nanshan in SON and DJF was higher than 0.001, with a significance level of 0.01.

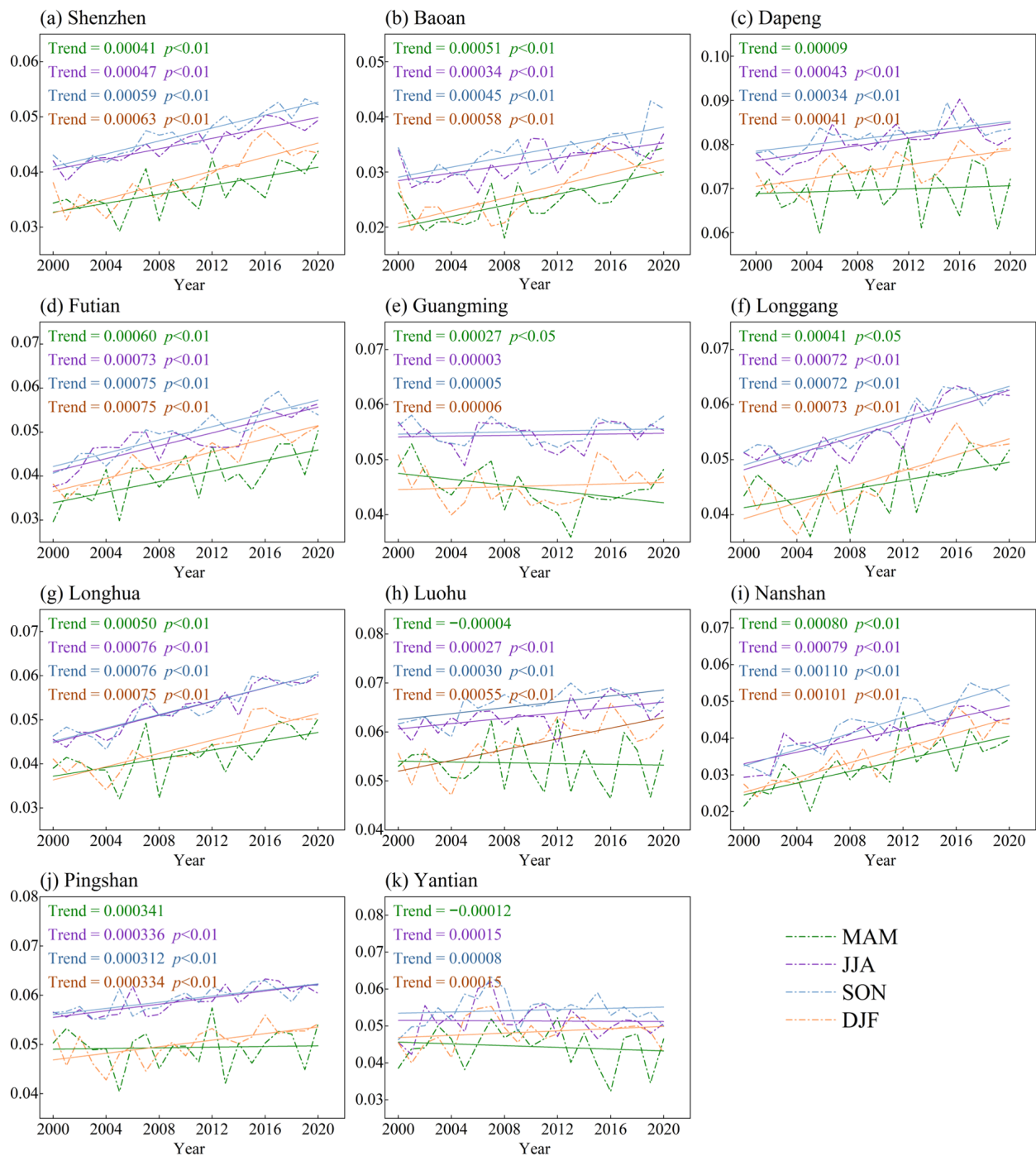


Figure 6. Changes in UG exposure in (a) Shenzhen, (b) Baoan, (c) Dapeng, (d) Futian, (e) Guangming, (f) Longgang, (g) Longhua, (h) Luohua, (i) Nanshan, (j) Pingshan, and (k) Yantian.

3.3. Inequality in Urban Greenspace Exposure in Shenzhen

The inequality of UG exposure in Shenzhen is shown in Figures 7 and A2. Of the four seasons, inequality was higher in MAM and DJF and lower in JJA and SON. In JJA, SON, and DJF, the largest spatial inequality was observed in 2001, with Gini indices of 0.160, 0.152, and 0.172, respectively. In MAM, the largest Gini index was observed in 2005, with a value of 0.182, which was also the highest among the four seasons during 2000–2020. The lowest values of UG exposure inequality were those in MAM and SON in 2019, JJA in 2020, and DJF in 2015. Overall, this inequality showed a downward trend in each season, although the rate of decline varied across the seasons. The inequality in MAM showed

the fastest rate of decline, followed by the inequality in DJF, whereas the inequality in JJA demonstrated the slowest rate of decline.

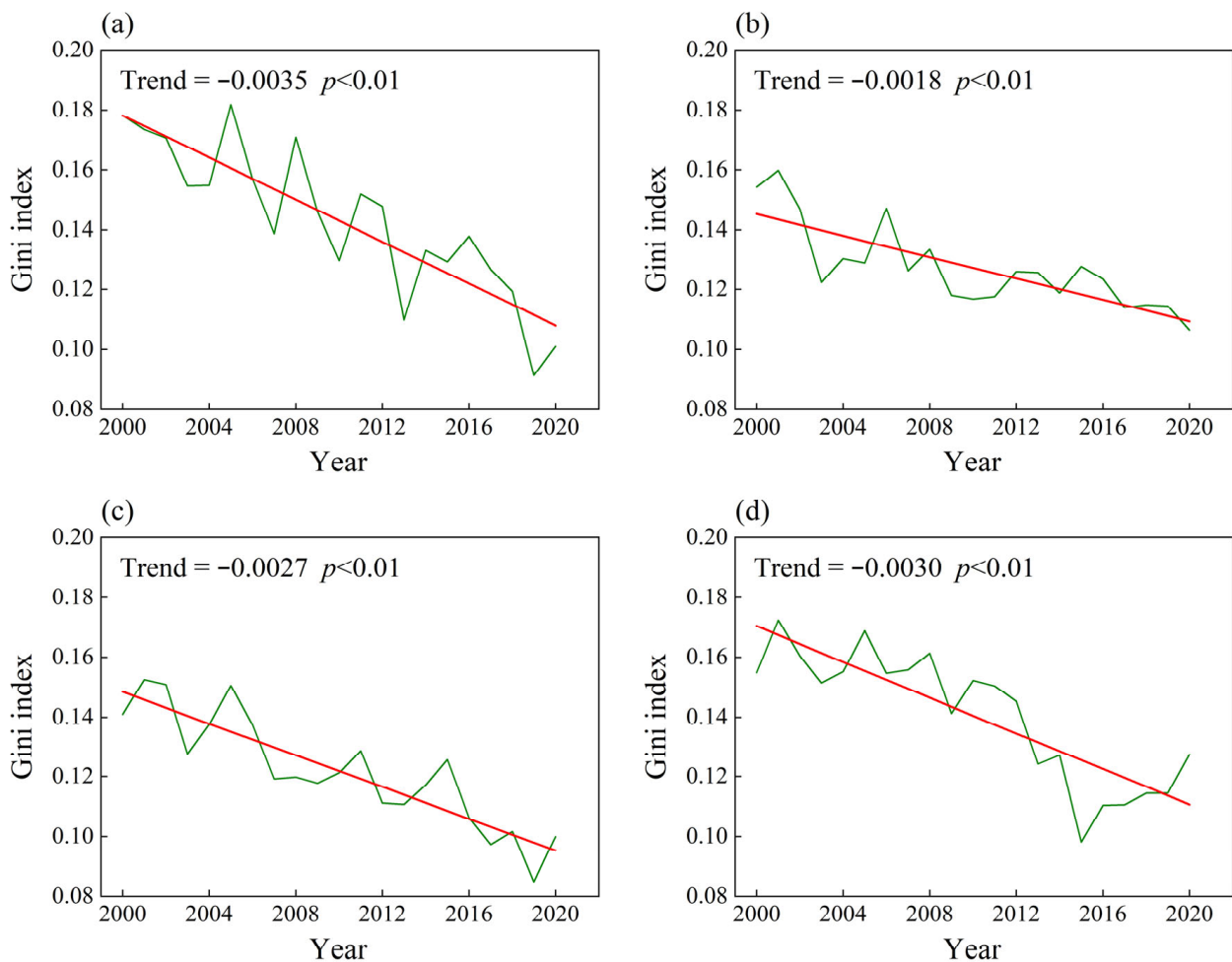


Figure 7. Changes in inequality regarding UG exposure in Shenzhen from 2000 to 2020 in (a) MAM, (b) JJA, (c) SON, and (d) DJF. The green and red lines represent the estimates of Gini index and the trends during the periods 2000–2020.

4. Discussion

In this study, we explored the spatiotemporal variation in UG in Shenzhen using long-term time-series data and quantified urban population-weighted greenspace exposure and inequality across seasons. We found that the urban greenspace coverage in Shenzhen gradually decreased from 2000 to 2020, but the rate of decline was faster and then slower, which may be attributed to the implementation of the “basic ecological control line” in the early 21st century, which aimed to restrict urban expansion in Shenzhen [54]. The distribution of UG in Shenzhen showed obvious spatial differences, and over the past 20 years, the reduction in UG was higher in the western part of Shenzhen than in the eastern part. The UG has become enlarged because of urban expansion. This is consistent with the finding that the direction of urban expansion in Shenzhen is eastward [55]. By contrast, eastern Shenzhen features a significant number of ecological reserves, resulting in less greenspace reduction. Notably, areas such as Wutong Mountain, located on the border of Longgang and Yantian, and Qiniang Mountain in Dapeng possess higher elevations and slopes, limiting the extent of urban expansion and preserving more UG. The establishment of Dapeng as an ecological protection zone in 2011 further supports this preservation effort. Studies have also shown that the habitat quality in Shenzhen has significantly deteriorated in recent years, with areas of high habitat quality primarily concentrated in the eastern

part of the city [29]. In addition, we found that the autumn NDVI of the UG in Shenzhen was relatively high, which may be related to the saturation of the NDVI in areas with high photosynthetic rates [56]. The small change in the NDVI trend in Dapeng may also be partially responsible for this. Notably, Guangming consistently showed a decreasing NDVI trend regardless of the season, which may be closely linked to urban construction activities. Recent studies have indicated that, although the equivalent area of ecological land is decreasing, the average quality of ecological land has improved [57]. In 2005, the Shenzhen Municipal Government implemented an urban growth boundary, altering the pattern of urban expansion towards inward regeneration, which led to negative NDVI trends in many areas [58–60]. Overall, the rapid urbanization process in Shenzhen has led to the expansion of built-up areas, resulting in a substantial reduction in UG. From 2000 to 2020, the built-up area of Shenzhen expanded from 330.5 square kilometers to more than 900 square kilometers. This rapid urbanization has altered existing land use patterns, consequently affecting the species composition of Shenzhen’s municipal parks [61]. Considering the decreasing amount of ecological land in Shenzhen, the government has implemented policies to improve the sustainability of land use and restrict the availability of land for development.

The UG exposure in Shenzhen shows a spatially decreasing trend from west to east. This is mainly because the eastern part of Shenzhen not only has more greenspace but also has a lower population density than the west. The southeastern part of Shenzhen is far from the administrative boundary of the city center, and planning focuses on urban ecosystem services, while the western part focuses more on economic development. In southeastern Shenzhen, which is predominantly covered by artificial evergreen forests, the UG exposure remained relatively stable throughout the year [62]. Therefore, in recent years, the center of the urban ecological land has gradually moved southeast [7,57]. Temporally, UG exposure was higher in JJA and SON than in MAM and DJF. Shenzhen has a subtropical monsoon climate, characterized by high temperatures and rainfall in JJA and lower temperatures and rainfall in DJF. Because of the lagging effect of climate on plant growth, the UG exposure of urban residents was higher in JJA and SON than in MAM and DJF. Over the years, as living standards have improved and demand for cultural services has increased, the UG exposure of urban residents in Shenzhen has gradually increased across all seasons. To address the inequality in UG exposure, future UG construction efforts should focus on western Shenzhen to increase UG exposure for residents in that area. This would contribute to reducing the disparities in UG exposure among different parts of the city.

Notably, the ten districts of Shenzhen differ in terms of geographical location and ecosystem characteristics. Furthermore, the regional development of these districts varies, leading to differences in UG exposure inequality [60]. In this investigation, we found that the inequality in UG exposure was higher in MAM and SON than in JJA and DJF. This phenomenon can be attributed to two possible reasons. First, the vegetation in MAM and DJF may not be as lush as that in JJA and SON. Second, the index used to measure UG exposure was the NDVI, which may be subject to saturation. In addition, we found that the rate of inequality in MAM declined the fastest over the 21 years investigated, which may be associated with phenological changes in urban vegetation. These factors contribute to the current state of inequality in UG exposure in Shenzhen. The decrease in inequality over the past two decades indicates that Shenzhen has made notable progress in UG development. Compared to other cities in China, Shenzhen’s Gini index is less than 0.2 and displays a downward trend, suggesting that the level of UG exposure inequality in Shenzhen is relatively low [37].

In the context of a healthy city, protecting the amount of greenspace and improving its quality can help to optimize the level of greenspace exposure and reduce inequality in greenspace. When formulating an urban greenspace planning scheme for Shenzhen based on our research, it is necessary to fully consider the spatial heterogeneity of Shenzhen’s UG. To protect greenspaces and improve their quality, greening modes in different regions should be determined according to local conditions. In addition, during the devel-

opment of Shenzhen, greenspace should be optimized based on scientific research and a dynamic population distribution model, and the layout of land use should be rationally distributed in different regions to improve residents' exposure to greenspace and reduce greenspace inequality.

5. Conclusions

In this study, we investigated the spatiotemporal patterns, population-weighted exposure, and inequality in urban greenspace (UG) in Shenzhen over the past two decades using gridded data (land cover, NDVI, and population). Our findings revealed that the UG area in Shenzhen has been decreasing in recent years, although the rate of decrease has slowed down. Owing to the area's unique climatic conditions, the NDVI of UG does not vary much between seasons, but there are some differences in the NDVI trends between seasons. By quantitatively assessing UG exposure, we found that although the overall UG exposure has increased in Shenzhen over the past two decades, the eastern part of the city has much higher UG exposure than the western part. However, the good news is that the inequality between the ten districts is decreasing each year. In the future, Shenzhen needs to improve its greenspace supply and create more greenspace in areas with low UG exposure to enhance the quality of human habitation and reduce inequality. This study expands our understanding of UG in Shenzhen and provides scientific methodological support for its sustainable development. Nevertheless, this study has some limitations, such as the lack of quantification of driving factors. In addition, the accuracy of remote sensing data may lead to errors in urban greenspace measurements. More high-resolution remote sensing datasets are required to explore subtle differences within a city and comprehensively assess UG quality.

Author Contributions: Conceptualization, Y.B.; methodology, Y.B.; software, Y.B. and M.L.; validation, M.L.; formal analysis, W.W.; investigation, S.L.; data curation, Y.B.; writing—original draft preparation, Y.B.; writing—review and editing, Y.B., M.L., W.W., X.X. and S.L.; visualization, X.X.; supervision, W.W.; project administration, X.X.; funding acquisition, S.L. All authors have read and agreed to the published version of the manuscript.

Funding: This research was funded by the Shenzhen Ecology and Environment National Observation and Research Station (Grant No. SZDL2023001063).

Data Availability Statement: The data presented in this study are available on request from the author.

Acknowledgments: This work was financially supported by the Maintenance Project of State Environmental Protection Scientific Observation and Research Station in Shenzhen.

Conflicts of Interest: The authors declare no conflict of interest.

Appendix A

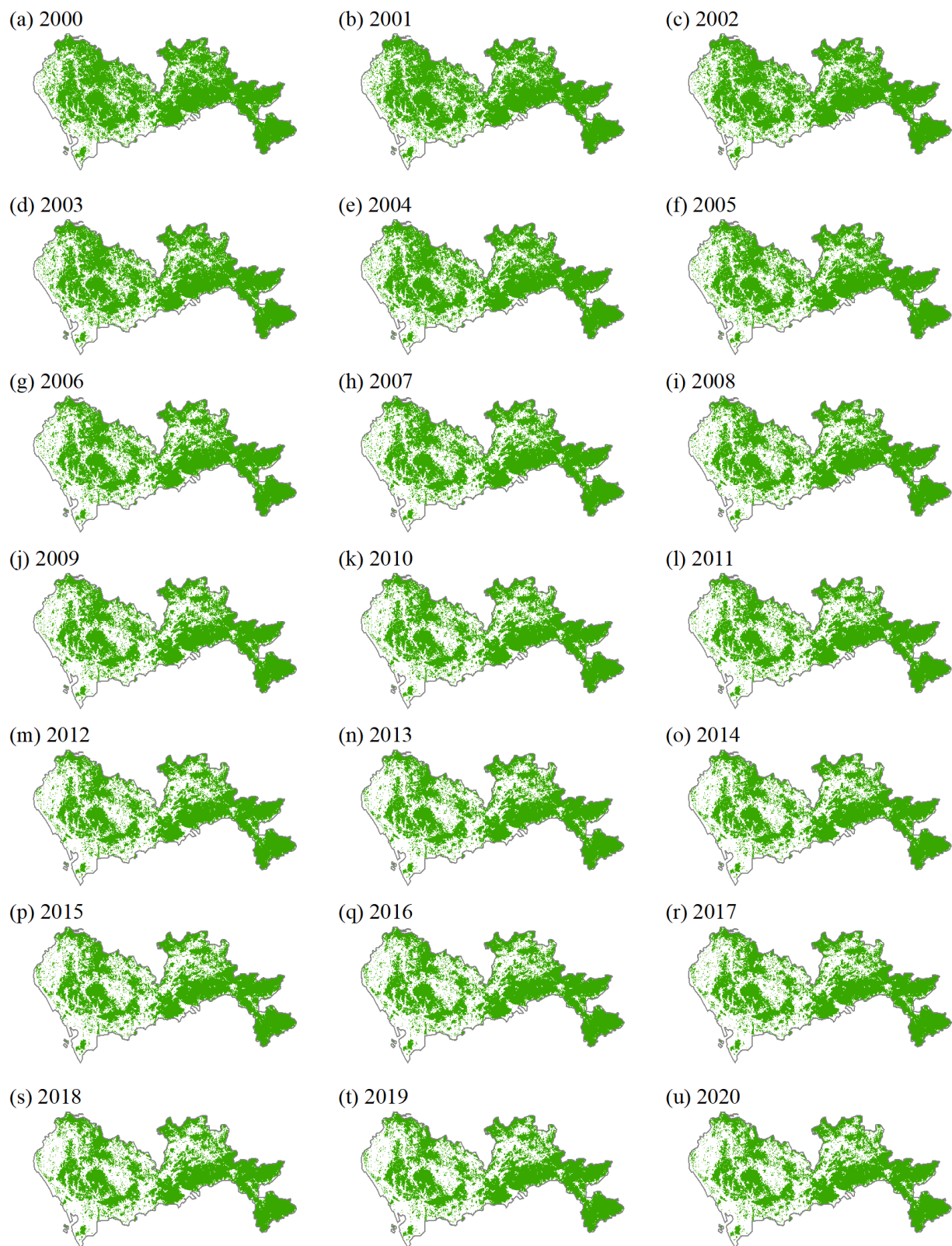


Figure A1. The spatial distribution of UG in Shenzhen (a–u) from 2000 to 2020.

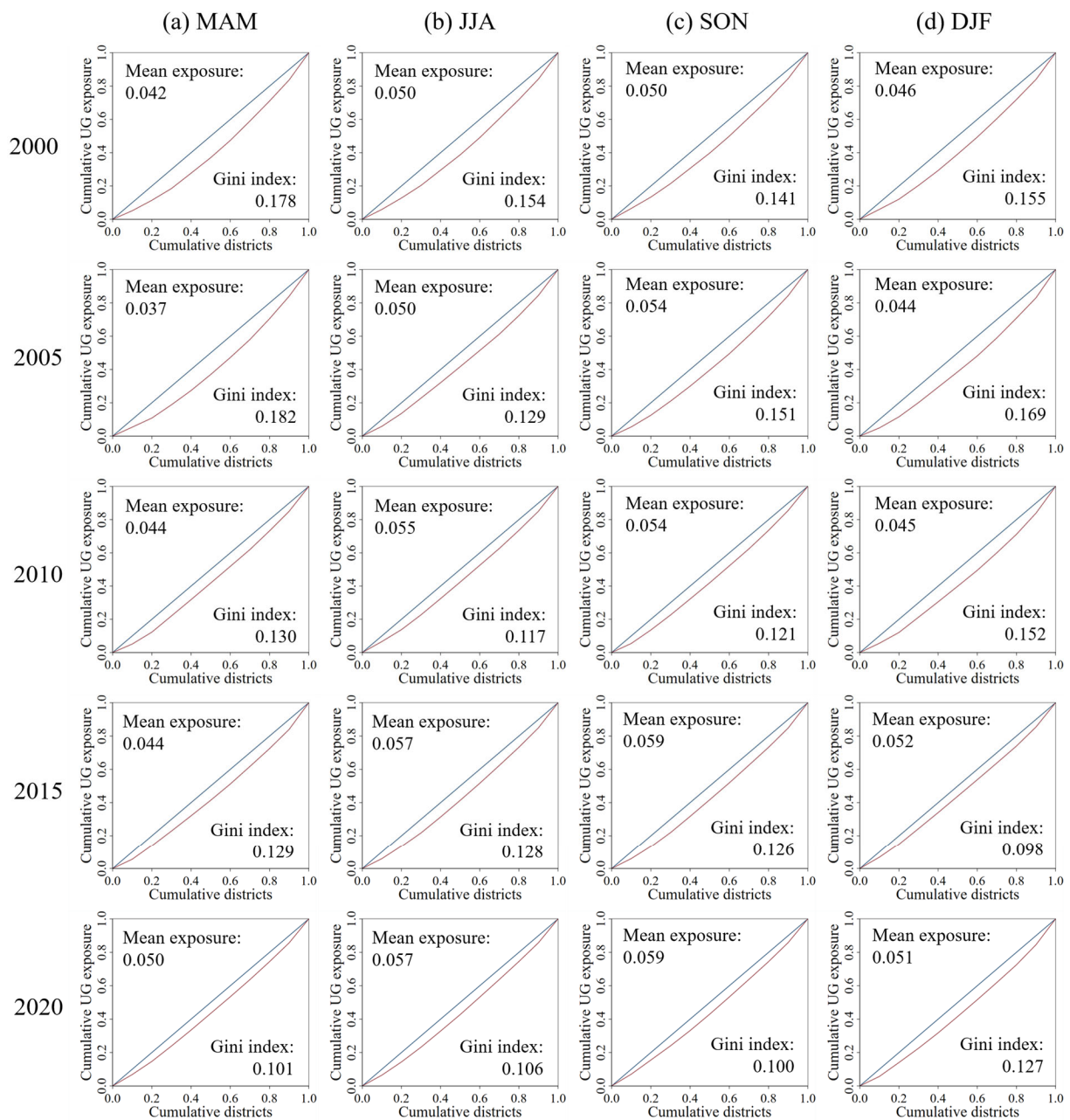


Figure A2. The Lorenz curves and Gini index of UG exposure in Shenzhen from 2000 to 2020 with five-year intervals (a) MAM, (b) JJA, (c) SON, (d) DJF. The 45-degree blue line represents absolute equality line. The red line represents the distribution of UG exposure.

References

1. Yang, L.; Zhao, S.; Liu, S. A global analysis of urbanization effects on amphibian richness: Patterns and drivers. *Glob. Environ. Chang.* **2022**, *73*, 102476. [[CrossRef](#)]
2. Zhou, W.; Yu, W.; Qian, Y.; Han, L.; Pickett, S.T.A.; Wang, J.; Li, W.; Ouyang, Z. Beyond city expansion: Multi-scale environmental impacts of urban megaregion formation in China. *Natl. Sci. Rev.* **2022**, *9*, nwab107. [[CrossRef](#)] [[PubMed](#)]
3. Bren d'Amour, C.; Reitsma, F.; Baiocchi, G.; Barthel, S.; Güneralp, B.; Erb, K.-H.; Haberl, H.; Creutzig, F.; Seto, K.C. Future urban land expansion and implications for global croplands. *Proc. Natl. Acad. Sci. USA* **2017**, *114*, 8939–8944. [[CrossRef](#)] [[PubMed](#)]
4. Zhao, S.; Zhou, D.; Zhu, C.; Sun, Y.; Wu, W.; Liu, S. Spatial and Temporal Dimensions of Urban Expansion in China. *Environ. Sci. Technol.* **2015**, *49*, 9600–9609. [[CrossRef](#)] [[PubMed](#)]
5. Jia, A.; Wang, D.; Liang, S.; Peng, J.; Yu, Y. Global Daily Actual and Snow-Free Blue-Sky Land Surface Albedo Climatology From 20-Year MODIS Products. *J. Geophys. Res. Atmos.* **2022**, *127*, e2021JD035987. [[CrossRef](#)]
6. Liu, M.; Ma, H.; Bai, Y. Understanding the Drivers of Land Surface Temperature Based on Multisource Data: A Spatial Econometric Perspective. *IEEE J. Sel. Top. Appl. Earth Obs. Remote Sens.* **2021**, *14*, 12263–12272. [[CrossRef](#)]

7. Li, H.; Zhou, W.; Wang, W.; Zheng, Z. Imbalanced supply and demand of temperature regulation service provided by urban forests: A case study in Shenzhen, China. *Ecol. Indic.* **2022**, *145*, 109666. [[CrossRef](#)]
8. Wang, J.; Zhou, W.; Wang, J. Time-Series Analysis Reveals Intensified Urban Heat Island Effects but without Significant Urban Warming. *Remote Sens.* **2019**, *11*, 2229. [[CrossRef](#)]
9. Jia, A.; Liang, S.; Wang, D. Generating a 2-km, all-sky, hourly land surface temperature product from Advanced Baseline Imager data. *Remote Sens. Environ.* **2022**, *278*, 113105. [[CrossRef](#)]
10. Wang, H.; Li, B.; Yi, T.; Wu, J. Heterogeneous Urban Thermal Contribution of Functional Construction Land Zones: A Case Study in Shenzhen, China. *Remote Sens.* **2022**, *14*, 1851. [[CrossRef](#)]
11. Dong, J.; Peng, J.; He, X.; Corcoran, J.; Qiu, S.; Wang, X. Heatwave-induced human health risk assessment in megacities based on heat stress-social vulnerability-human exposure framework. *Landsc. Urban Plan.* **2020**, *203*, 103907. [[CrossRef](#)]
12. World Health, O. Shanghai Consensus on Healthy Cities 2016. *Health Promot. Int.* **2017**, *32*, 603–605. [[CrossRef](#)]
13. Massaro, E.; Schifanella, R.; Piccardo, M.; Caporaso, L.; Taubenbock, H.; Cescatti, A.; Duveiller, G. Spatially-optimized urban greening for reduction of population exposure to land surface temperature extremes. *Nat. Commun.* **2023**, *14*, 2903. [[CrossRef](#)] [[PubMed](#)]
14. Adams, M.P.; Smith, P.L. A systematic approach to model the influence of the type and density of vegetation cover on urban heat using remote sensing. *Landsc. Urban Plan.* **2014**, *132*, 47–54. [[CrossRef](#)]
15. Kong, F.; Yin, H.; James, P.; Hutyrá, L.R.; He, H.S. Effects of spatial pattern of greenspace on urban cooling in a large metropolitan area of eastern China. *Landsc. Urban Plan.* **2014**, *128*, 35–47. [[CrossRef](#)]
16. Maes, M.J.A.; Pirani, M.; Booth, E.R.; Shen, C.; Milligan, B.; Jones, K.E.; Toledano, M.B. Benefit of woodland and other natural environments for adolescents' cognition and mental health. *Nat. Sustain.* **2021**, *4*, 851–858. [[CrossRef](#)]
17. Mueller, N.; Rojas-Rueda, D.; Khreis, H.; Cirach, M.; Andres, D.; Ballester, J.; Bartoll, X.; Daher, C.; Deluca, A.; Echave, C.; et al. Changing the urban design of cities for health: The superblock model. *Env. Int.* **2020**, *134*, 105132. [[CrossRef](#)]
18. Tost, H.; Reichert, M.; Braun, U.; Reinhard, I.; Peters, R.; Lautenbach, S.; Hoell, A.; Schwarz, E.; Ebner-Priemer, U.; Zipf, A.; et al. Neural correlates of individual differences in affective benefit of real-life urban green space exposure. *Nat. Neurosci.* **2019**, *22*, 1389–1393. [[CrossRef](#)]
19. Wang, J.; Wang, W.; Zhang, S.; Wang, Y.; Sun, Z.; Wu, B. Spatial and temporal changes and development predictions of urban green spaces in Jinan City, Shandong, China. *Ecol. Indic.* **2023**, *152*, 110373. [[CrossRef](#)]
20. Liao, Y.; Wang, J.; Meng, B.; Li, X. Integration of GP and GA for mapping population distribution. *Int. J. Geogr. Inf. Sci.* **2010**, *24*, 47–67. [[CrossRef](#)]
21. Zhou, Y.; Shi, T.; Hu, Y.; Gao, C.; Liu, M.; Fu, S.; Wang, S. Urban green space planning based on computational fluid dynamics model and landscape ecology principle: A case study of Liaoyang City, Northeast China. *Chin. Geogr. Sci.* **2011**, *21*, 465–475. [[CrossRef](#)]
22. Chen, B.; Wu, S.; Song, Y.; Webster, C.; Xu, B.; Gong, P. Contrasting inequality in human exposure to greenspace between cities of Global North and Global South. *Nat. Commun.* **2022**, *13*, 4636. [[CrossRef](#)]
23. Chen, B.; Tu, Y.; Wu, S.; Song, Y.; Jin, Y.; Webster, C.; Xu, B.; Gong, P. Beyond green environments: Multi-scale difference in human exposure to greenspace in China. *Environ. Int.* **2022**, *166*, 107348. [[CrossRef](#)] [[PubMed](#)]
24. Liu, M.; Li, L.; Li, Q.; Bai, Y.; Hu, C. Pedestrian Flow Prediction in Open Public Places Using Graph Convolutional Network. *ISPRS Int. J. Geo. Inf.* **2021**, *10*, 455. [[CrossRef](#)]
25. Ding, K.; Huang, Y.; Wang, C.; Li, Q.; Yang, C.; Fang, X.; Tao, M.; Xie, R.; Dai, M. Time Series Analysis of Land Cover Change Using Remotely Sensed and Multisource Urban Data Based on Machine Learning: A Case Study of Shenzhen, China from 1979 to 2022. *Remote Sens.* **2022**, *14*, 5706. [[CrossRef](#)]
26. Shi, P.; Yu, D. Assessing urban environmental resources and services of Shenzhen, China: A landscape-based approach for urban planning and sustainability. *Landsc. Urban Plan.* **2014**, *125*, 290–297. [[CrossRef](#)]
27. Hong, W.; Guo, R.; Su, M.; Tang, H.; Chen, L.; Hu, W. Sensitivity evaluation and land-use control of urban ecological corridors: A case study of Shenzhen, China. *Land Use Policy* **2017**, *62*, 316–325. [[CrossRef](#)]
28. Liu, L.; Lin, Y.; Wang, L.; Cao, J.; Wang, D.; Xue, P.; Liu, J. An integrated local climatic evaluation system for green sustainable eco-city construction: A case study in Shenzhen, China. *Build. Environ.* **2017**, *114*, 82–95. [[CrossRef](#)]
29. Liu, Z.; Liu, Z.; Zhou, Y.; Huang, Q. Distinguishing the Impacts of Rapid Urbanization on Ecosystem Service Trade-Offs and Synergies: A Case Study of Shenzhen, China. *Remote Sens.* **2022**, *14*, 4604. [[CrossRef](#)]
30. Tian, S.; Zhang, Y.; Xu, Y.; Wang, Q.; Yuan, X.; Ma, Q.; Chen, L.; Ma, H.; Xu, Y.; Yang, S.; et al. Urban ecological security assessment and path regulation for ecological protection—A case study of Shenzhen, China. *Ecol. Indic.* **2022**, *145*, 109717. [[CrossRef](#)]
31. Zeng, Q.; Xie, Y.; Liu, K. Assessment of the patterns of urban land covers and impervious surface areas: A case study of Shenzhen, China. *Phys. Chem. Earth Parts A/B/C* **2019**, *110*, 1–7. [[CrossRef](#)]
32. Peng, J.; Liu, Y.; Wu, J.; Lv, H.; Hu, X. Linking ecosystem services and landscape patterns to assess urban ecosystem health: A case study in Shenzhen City, China. *Landsc. Urban Plan.* **2015**, *143*, 56–68. [[CrossRef](#)]
33. Qian, Y.; Chen, Y.; Lin, C.; Wang, W.; Zhou, W. Revealing patterns of greenspace in urban areas resulting from three urban growth types. *Phys. Chem. Earth Parts A/B/C* **2019**, *110*, 14–20. [[CrossRef](#)]
34. Zhang, L.; Chen, P.; Hui, F. Refining the accessibility evaluation of urban green spaces with multiple sources of mobility data: A case study in Shenzhen, China. *Urban For. Urban Green.* **2022**, *70*, 127550. [[CrossRef](#)]
35. Hong, W.; Guo, R.; Tang, H. Potential assessment and implementation strategy for roof greening in highly urbanized areas: A case study in Shenzhen, China. *Cities* **2019**, *95*, 102468. [[CrossRef](#)]

36. Yang, J.; Huang, X. The 30 m annual land cover dataset and its dynamics in China from 1990 to 2019. *Earth Syst. Sci. Data* **2021**, *13*, 3907–3925. [[CrossRef](#)]
37. Song, Y.; Chen, B.; Ho, H.C.; Kwan, M.P.; Liu, D.; Wang, F.; Wang, J.; Cai, J.; Li, X.; Xu, Y.; et al. Observed inequality in urban greenspace exposure in China. *Environ. Int.* **2021**, *156*, 106778. [[CrossRef](#)] [[PubMed](#)]
38. Walther, S.; Voigt, M.; Thum, T.; Gonsamo, A.; Zhang, Y.; Köhler, P.; Jung, M.; Varlagin, A.; Guanter, L. Satellite chlorophyll fluorescence measurements reveal large-scale decoupling of photosynthesis and greenness dynamics in boreal evergreen forests. *Glob. Chang. Biol.* **2016**, *22*, 2979–2996. [[CrossRef](#)] [[PubMed](#)]
39. Gao, J.; Shi, Y.; Zhang, H.; Chen, X.; Zhang, W.; Shen, W.; Xiao, T.; Zhang, Y. China Regional 250 m Normalized Difference Vegetation Index Data Set (2000–2022). Available online: <https://cstr.cn/18406.11.Terre.tpd.300328> (accessed on 10 July 2023).
40. Center for International Earth Science Information Network—C.C.U. *Gridded Population of the World, Version 4 (GPWv4)*; Population Count Revision 11; NASA Socioeconomic Data and Applications Center (SEDAC): Palisades, NY, USA, 2018.
41. Kendall, M.G. *Rank Correlation Methods*; Griffin: Oxford, UK, 1948.
42. Sen, P.K. Estimates of the regression coefficient based on Kendall's tau. *J. Am. Stat. Assoc.* **1968**, *63*, 1379–1389. [[CrossRef](#)]
43. Bai, Y.; Li, S. Growth peak of vegetation and its response to drought on the Mongolian Plateau. *Ecol. Indic.* **2022**, *141*, 109150. [[CrossRef](#)]
44. Wei, W.; Zhang, H.; Ma, L.; Wang, X.; Guo, Z.; Xie, B.; Zhou, J.; Wang, J. Reconstruction and application of the temperature-precipitation-drought index in mainland China based on remote sensing datasets and a spatial distance model. *J. Environ. Manag.* **2022**, *323*, 116208. [[CrossRef](#)] [[PubMed](#)]
45. Zhou, Z.; Liu, S.; Ding, Y.; Fu, Q.; Wang, Y.; Cai, H.; Shi, H. Assessing the responses of vegetation to meteorological drought and its influencing factors with partial wavelet coherence analysis. *J. Environ. Manag.* **2022**, *311*, 114879. [[CrossRef](#)] [[PubMed](#)]
46. Zhao, A.; Tian, X.; Jin, Z.; Zhang, A. The imprint of urbanization on vegetation in the ecologically fragile area: A case study from China's Loess Plateau. *Ecol. Indic.* **2023**, *154*, 110791. [[CrossRef](#)]
47. Chen, B.; Song, Y.; Kwan, M.-P.; Huang, B.; Xu, B. How do people in different places experience different levels of air pollution? Using worldwide Chinese as a lens. *Environ. Pollut.* **2018**, *238*, 874–883. [[CrossRef](#)]
48. Song, Y.; Huang, B.; Cai, J.; Chen, B. Dynamic assessments of population exposure to urban greenspace using multi-source big data. *Sci. Total Environ.* **2018**, *634*, 1315–1325. [[CrossRef](#)]
49. Jbaily, A.; Zhou, X.; Liu, J.; Lee, T.-H.; Kamareddine, L.; Verguet, S.; Dominici, F. Air pollution exposure disparities across US population and income groups. *Nature* **2022**, *601*, 228–233. [[CrossRef](#)]
50. Kyaw, A.K.; Hamed, M.M.; Kamruzzaman, M.; Shahid, S. Spatiotemporal changes in population exposure to heat stress in South Asia. *Sustain. Cities Soc.* **2023**, *93*, 104544. [[CrossRef](#)]
51. Shen, H.; Shen, G.; Chen, Y.; Russell, A.G.; Hu, Y.; Duan, X.; Meng, W.; Xu, Y.; Yun, X.; Lyu, B.; et al. Increased air pollution exposure among the Chinese population during the national quarantine in 2020. *Nat. Hum. Behav.* **2021**, *5*, 239–246. [[CrossRef](#)]
52. Wolff, N.H.; Zepetello, L.R.V.; Parsons, L.A.; Aggraeni, I.; Battisti, D.S.; Ebi, K.L.; Game, E.T.; Kroeger, T.; Masuda, Y.J.; Spector, J.T. The effect of deforestation and climate change on all-cause mortality and unsafe work conditions due to heat exposure in Berau, Indonesia: A modelling study. *Lancet Planet. Health* **2021**, *5*, e882–e892. [[CrossRef](#)] [[PubMed](#)]
53. Liu, M.; Fang, C.; Bai, Y.; Sun, B.; Liao, X.; Liu, Z. Regional inequality and urban-rural difference of dietary water footprint in China. *Resour. Conserv. Recycl.* **2023**, *199*, 107236. [[CrossRef](#)]
54. Qian, Y.; Zhou, W.; Pickett, S.T.A.; Yu, W.; Xiong, D.; Wang, W.; Jing, C. Integrating structure and function: Mapping the hierarchical spatial heterogeneity of urban landscapes. *Ecol. Process.* **2020**, *9*, 59. [[CrossRef](#)]
55. Meng, L.; Sun, Y.; Zhao, S. Comparing the spatial and temporal dynamics of urban expansion in Guangzhou and Shenzhen from 1975 to 2015: A case study of pioneer cities in China's rapid urbanization. *Land Use Policy* **2020**, *97*, 104753. [[CrossRef](#)]
56. Bai, Y.; Li, S.; Zhou, J.; Liu, M.; Guo, Q. Revisiting vegetation activity of Mongolian Plateau using multiple remote sensing datasets. *Agric. For. Meteorol.* **2023**, *341*, 109649. [[CrossRef](#)]
57. Peng, J.; Zhao, M.; Guo, X.; Pan, Y.; Liu, Y. Spatial-temporal dynamics and associated driving forces of urban ecological land: A case study in Shenzhen City, China. *Habitat Int.* **2017**, *60*, 81–90. [[CrossRef](#)]
58. Hao, P.; Sliuzas, R.; Geertman, S. The development and redevelopment of urban villages in Shenzhen. *Habitat Int.* **2011**, *35*, 214–224. [[CrossRef](#)]
59. Qian, J.; Peng, Y.; Luo, C.; Wu, C.; Du, Q. Urban Land Expansion and Sustainable Land Use Policy in Shenzhen: A Case Study of China's Rapid Urbanization. *Sustainability* **2015**, *8*, 16. [[CrossRef](#)]
60. Yu, W.; Zhang, Y.; Zhou, W.; Wang, W.; Tang, R. Urban expansion in Shenzhen since 1970s: A retrospect of change from a village to a megacity from the space. *Phys. Chem. Earth Parts A/B/C* **2019**, *110*, 21–30. [[CrossRef](#)]
61. Ye, Y.; Lin, S.; Wu, J.; Li, J.; Zou, J.; Yu, D. Effect of rapid urbanization on plant species diversity in municipal parks, in a new Chinese city: Shenzhen. *Acta Ecol. Sin.* **2012**, *32*, 221–226. [[CrossRef](#)]
62. Shu, C.; Cai, W.; Han, B.; Li, X.; Jiang, N.; Ouyang, Z. A study on the characteristics of the dominant vegetation species in Shenzhen based on a rapid census method. *Acta Ecol. Sin.* **2020**, *40*, 8516–8527. [[CrossRef](#)]

Disclaimer/Publisher's Note: The statements, opinions and data contained in all publications are solely those of the individual author(s) and contributor(s) and not of MDPI and/or the editor(s). MDPI and/or the editor(s) disclaim responsibility for any injury to people or property resulting from any ideas, methods, instructions or products referred to in the content.